

3. Equilibrium tidal theory

3.1 Definition and development of equilibrium tidal theory

The equilibrium tidal theory is based on the assumption that pressure and gravitation forces are always in full balance. As a result we don't have relative acceleration and hence no relative velocities due to tidal forcing. Necessary conditions are, (i) water movement is not restricted by boundaries, hence we assume a fully water-covered earth and (ii) dynamic aspects of the earth rotation relative to the deformed water surface are small compared to pressure and gravitation forces. Hence, it follows that the water has to be of sufficient depth to avoid that the turbulent bottom boundary layer, which exists independently of water depth for tidal waves (body force), may disturb the water movements significantly. Mass transport can occur only with minimum speed to fulfil the assumption of non-acceleration conditions.

These assumptions can be resumed in the following equation (using a potential for the gravitational force):

$$0 = -\alpha \nabla p - \nabla \phi_g - \nabla \phi_t \quad (77)$$

With the tidal potential ϕ_t and the gravitational potential from the earth being ϕ_g . The specific volume α is assumed to be a constant. We therefore can re-write the equation as (summarize the potentials):

$$0 = -\nabla(\alpha p + \phi_g + \phi_t) \quad (78)$$

and hence it follows that

$$C = -\alpha p - \phi_g - \phi_t \quad (79)$$

is constant for the whole ocean. Under assumption of constant atmospheric pressure p_0 this results for the sea surface in

$$C_2 = \phi_g + \phi_t \quad (80)$$

i.e. the sum of gravitational potential and tidal potential has to be const. every where on ocean surface. For the sea surface the following equation is valid:

$$r = a + \xi \quad (81)$$

Hence the gravitational potential is:

$$\phi_g = \frac{-GM_T}{a + \xi} + \text{const} = \frac{-GM_T}{a(1 + \xi/a)} + \text{const} \quad (82)$$

Power series expansion and higher order terms equalling zero results in:

$$\phi_g = g\xi - \frac{GM_T}{a} + const \quad (83)$$

We can use this equation to investigate the tidally induced sea surface elevation for an equilibrium earth, and compare surface elevation resulting from lunar- and solar- forcing. The vertical displacement of the sea surface can than be expressed by:

$$g\xi - \phi_i = const \quad (84)$$

If we integrate the tidal potential (33) we can show that the surface integral of the tidal potential vanish, since the tidal potential is mirror symmetric (assume earth is a sphere) with respect to the plane crossing the earth centre and the poles:

$$\iint_{\sigma} \phi_i d\sigma = 0 \quad (85)$$

The same is true for the integral over the surface elevation, since the mean surface elevation is zero (per definition)

$$\iint_{\sigma} \xi d\sigma = 0 \quad (86)$$

Consequently, the constant in (84) equals zero. This allows for approximation of the elevations from moon and suns tidal forcing respectively. Using 33 (i.e. the tidal potential as derived) and replacing r with a (av. radius) the following equations for the surface elevations resulting from sun and moons tidal potential can be derived:

$$\xi_L = -\frac{1}{g} \phi_{tL} \approx \frac{3}{2} \frac{M_L}{M_T} \frac{a^4}{R_L^3} \left(\cos^2 \theta_L - \frac{1}{3} \right) \quad (87)$$

$$\xi_S = -\frac{1}{g} \phi_{tS} \approx \frac{3}{2} \frac{M_S}{M_T} \frac{a^4}{R_S^3} \left(\cos^2 \theta_S - \frac{1}{3} \right) \quad (88)$$

Using these, we can develop the expressions for the surface elevation further and estimate the maximum elevations. We have to consider the following:

$$\frac{M_L}{M_T} = \frac{1}{81,5}; R_L = 60a \quad (89)$$

and

$$\frac{M_S}{M_T} = \frac{1}{3,33 \times 10^5}; R_S = 2,35 \times 10^4 a \quad (90)$$

and get:

$$\xi_L = 53,5 \left(\cos^2 \theta_L - \frac{1}{3} \right) cm \quad (91)$$

$$\xi_S = 24,6 \left(\cos^2 \theta_S - \frac{1}{3} \right) cm \quad (92)$$

The respective maximum elevations occurs if $\theta = 0$, i.e. in the intersection point for the central line and the earth surface. The relation of the maximum elevations resulting from sun and moons tidal forcing is equal to

$$\frac{\xi_S}{\xi_L} = 0,46 \quad (93)$$

The maximum elevations are

$$\xi_L = 35,7 cm \quad (94)$$

$$\xi_S = 16,4 cm \quad (95)$$

With $\theta = \pi / 2$ we get the elevation at the great circle normal to the central line. Here we can find the lowest surface elevation during the tidal cycle (low water):

$$\xi_L = -17,8 cm \quad (96)$$

$$\xi_S = -8,2 cm \quad (97)$$

The maximum elevation (high water) can be found in 2 pols with maxima in line with the central line. Low water is found in a broad belt around the earth with no elevation for $\theta = 55$ and $\theta = 125$ degree.

The equilibrium theory results in the right order of magnitude, however, it fails in a number of other substantial aspects, caused by a number of assumptions which are not fulfilled in reality. First of all, (i) the type of tidal wave defines the propagation speed. The wave speed of any wave longer than a few kilometres is limited to 230 m/s ($c = \sqrt{gd}$). This is only about half of the speed of the surface of the rotating earth to the moon (448m/s). Hence, the tidal waves, which manifest as shallow water waves, will not be able to follow the earth rotation, and hence, are not in equilibrium. (ii) Furthermore the presence of land masses hinders mass transport and (iii) all lateral movements are influenced by the earth rotation and will be deflected from the direction of forcing.

3.2 Physical explanation of equilibrium deformation and daily un-equality.

The equilibrium tidal theory explains an equilibrium deformation of sea level which is rotationally symmetric around the central line (shortest line from investigated point on earth and the respective celestial body). The deformation is furthermore mirror symmetric around the plane lying normal to the central line and the crossing the centre of the earth. The deformed sea surface forms an ellipsoid with one pole towards the celestial body (zenith) and the other pole diametrically opposed (nadir) (Fig. 20). This paradox result is explained by the tidal force balance (Figure 10), resulting in maximum tidal forces in the points nearest to the celestial body (zenith) and the point most far away (nadir), with gravitational attraction being larger in the zenith and centrifugal force being larger in nadir. In the centre of earth, gravitational and centrifugal force balance and no net resulting force exists here, this follows implicitly from stationary joint rotation of the 2 celestial bodies.

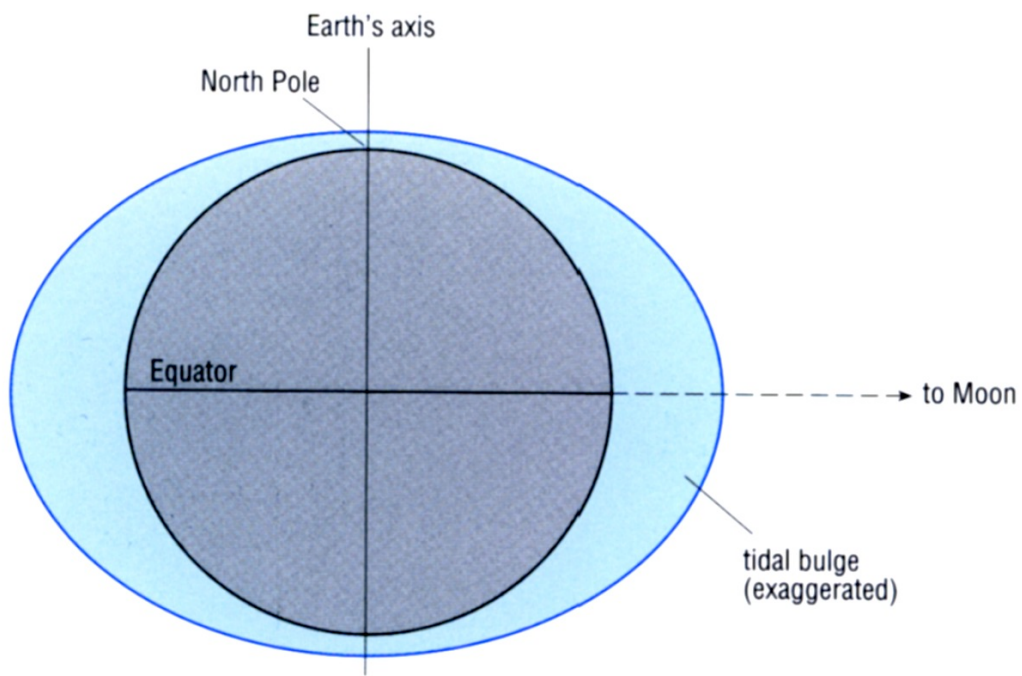


Figure 20. Tidal bulge as explained by equilibrium tidal theory. Figure taken from Open University Courses, Waves, Tides and Shallow water processes.

For development of tidal forces, we neglected the rotation of the earth round its own centre of mass and concentrated only on the revolution without rotation, i.e. the joint rotation of the earth and moon system around their joint centre of mass. The earth rotation round its own centre of mass does not act on the tidal force balance. However, it is responsible for the tidal phenomena on earth, i.e. the coming and going high and low water. We can illustrate this based on the equilibrium tidal deformation as developed from equilibrium tidal theory, if we combine the different rotation (earth rotation round its own axis) and translation (revolution without rotation), imaging the equilibrium deformation as being constant with respect to the moons (suns) position and consider a point on earth moving while rotating from high water to low water and again to high water while performing a half rotation.

Using this concept, we can as well understand the phenomena of daily inequality in tidal elevations (Figure 7) when semi-diurnal signals are dominant. In Figure 21 the tidal bulge as estimated from equilibrium tidal theory is displayed with respect to the equatorial plane.

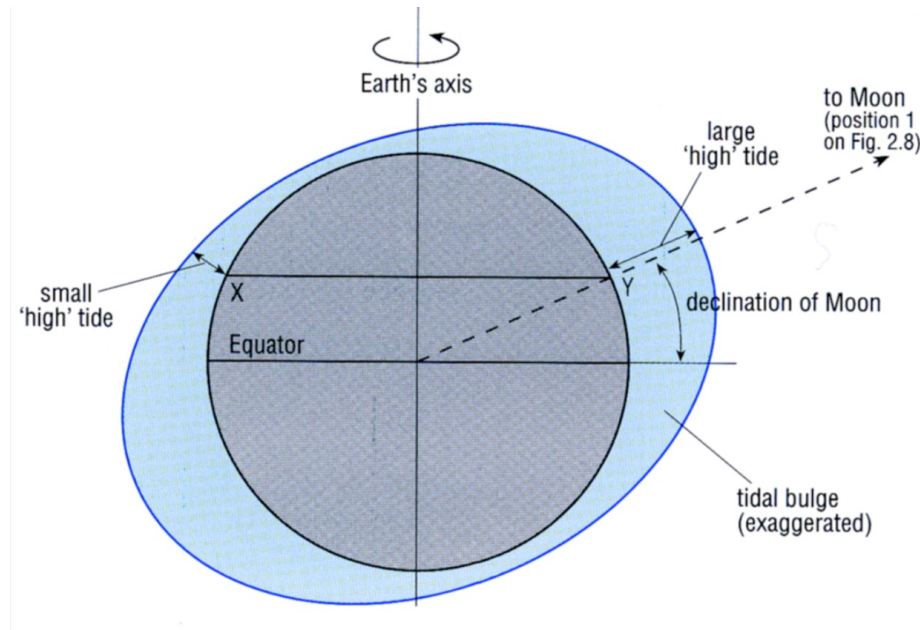


Figure 21. Tidal bulge in respect to the equatorial plane. Figure taken from Open University Courses, Waves, Tides and Shallow water processes.

In accordance with Figure 21, we can interpret the daily inequality as the result of the inclination of the equilibrium tidal bulge with the equatorial plane. As a consequence, any point on earth is

passing one ‘high high-tide’ elevation and one ‘low high-tide’ during one rotation of the earth round itself.

From Figure 21 (and our previous analysis) it is clear that the strength of the daily inequality depends on both, declination as well as geographical latitude. Daily inequality from the moon disappears when declination is zero. This happens when the moon is passing the equatorial plane, hence every 14 days. The declination is getting maximal ca .7 days later. For the sun, the daily inequality varies with a half year period (sun passing the equatorial plane). We can identify the intensity of the daily inequality for different latitudes, using the original form of the tidal potential and use (48) $\rightarrow \cos \theta = \cos \varphi \cos \psi \cos \delta + \sin \varphi \sin \delta$.

This results in tidal elevation described as proportional to

$$\cos^2 \theta = (\cos \varphi \cos \psi \cos \delta)^2 + 2 \cos \varphi \cos \psi \cos \delta \sin \varphi \sin \delta + (\sin \varphi \sin \delta)^2 \quad (98)$$

The term introducing the daily un-equality is $\cos \varphi \cos \psi \cos \delta \sin \varphi \sin \delta$, which is either positive or negative for nadir or zenith points. Hence, the dependence of daily inequality from latitude is described by $\cos \varphi \sin \varphi$, which implies that we’ll have no daily un-equality for the equatorial latitude (similarly the poles do not show daily un-equality, but as discussed before, they don’t show a semidiurnal signal).

3.3 Superposition of tidal forcing from moon and sun

Previous discussions and separate discussion of tidal potential did not display the characteristic feature existing because of the superposition of the two. We discussed the forcing terms in the form of the tidal potentials, but considered sun and moon separately. In this section we concentrate on the superposition of both signals and its consequences for the surface elevation.

The moons rotation round the earth takes 27,321 d (sideric month). After this period, the moon has not reached the same position to the soon, since the earth moon system has moved on its path around the sun. This only happens after 29,53 d (synodisc month), consequently this is the period between 2 full moon or 2 new moon events.

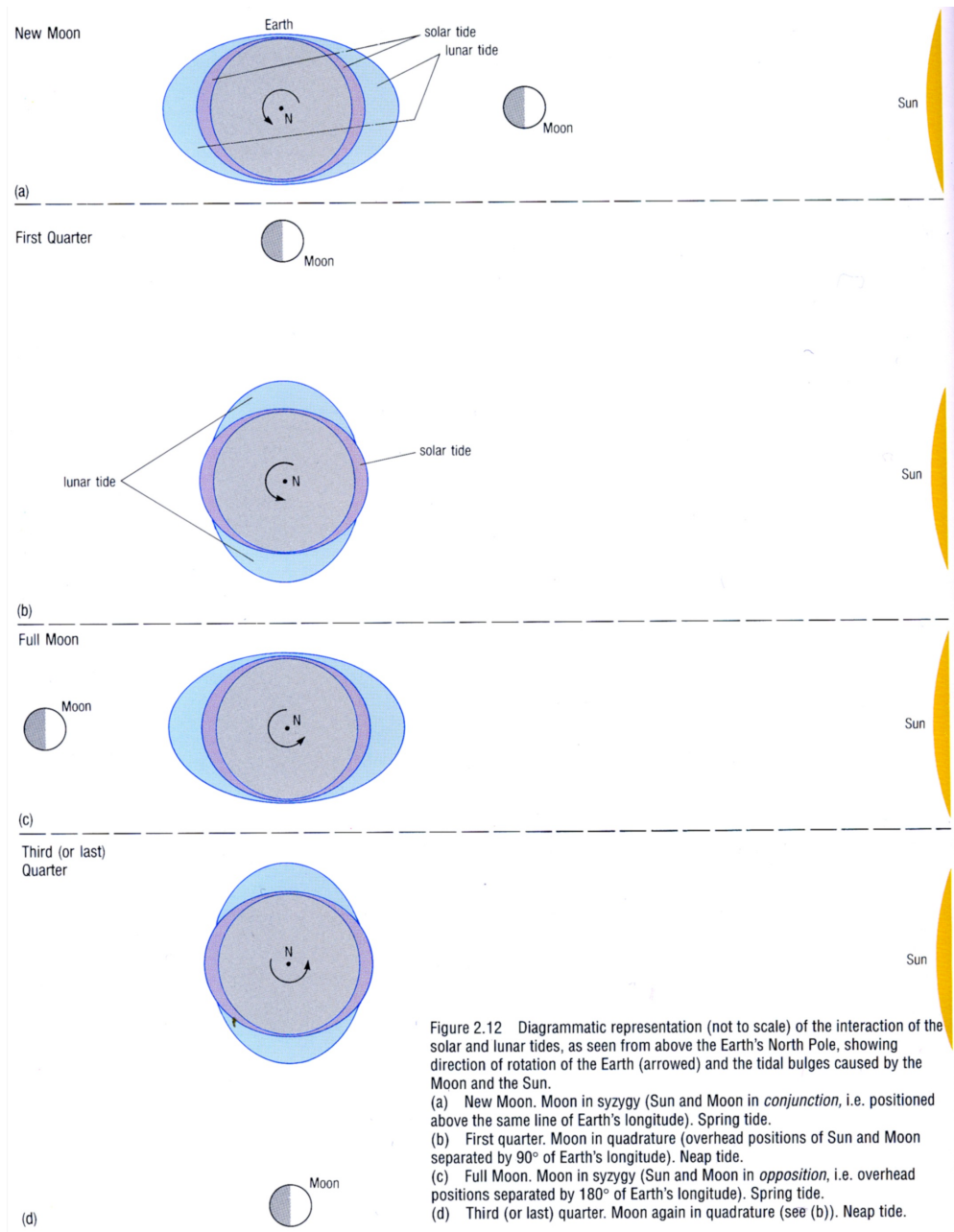


Figure 2.12 Diagrammatic representation (not to scale) of the interaction of the solar and lunar tides, as seen from above the Earth's North Pole, showing direction of rotation of the Earth (arrowed) and the tidal bulges caused by the Moon and the Sun.

- (a) New Moon. Moon in syzygy (Sun and Moon in *conjunction*, i.e. positioned above the same line of Earth's longitude). Spring tide.
- (b) First quarter. Moon in quadrature (overhead positions of Sun and Moon separated by 90° of Earth's longitude). Neap tide.
- (c) Full Moon. Moon in syzygy (Sun and Moon in *opposition*, i.e. overhead positions separated by 180° of Earth's longitude). Spring tide.
- (d) Third (or last) quarter. Moon again in quadrature (see (b)). Neap tide.

Figure 22. Interaction of solar and lunar tidal forcing. Figure taken from Open University Courses, Waves, Tides and Shallow water processes.

During new moon (sun and moon in conjunction) and full moon (sun and moon in opposition), the tidal forces from sun and moon add together due to the symmetric distribution of the tidal potential (and tidal bulge) with respect to zenith and nadir point. Consequently, a maximum tidal elevation (spring tide) will occur (Figure 22). In the first and third quarter the tidal forces

from sun and moon act against each other and a minimum tidal elevation results (neap tide). A spring tide results in approximately 3 times larger tidal elevations than compared to a neap tide. The modulation is approximately 14-daily and has the angular velocity of $2(s-\varepsilon)=2(0.549-0.041)$ (\rightarrow synodisc period). The angular frequency results from a difference between sun- and moon rotation velocity $2(\gamma-\varepsilon)$ and $2(\gamma-s)$, respectively.

3.4 Further analysis of spring-neap variations

The coupling between sun and moon results not only in a variation tidal elevation height, but also in a perturbation of the timing of high and low water, which will be illustrated by the following analysis.

We are introducing 2 new angular velocities σ and β defined as:

$$\text{Moons angular velocity } \sigma = 2(\gamma - s) \quad (102)$$

$$\text{Suns angular velocity } \sigma + \beta = 2(\gamma - \varepsilon) \quad (103)$$

with $\beta=2(s-\varepsilon)=2(0.549-0.041)=1.016$ degree/h and $\sigma=2(15.041-0.549)=28.984$ degree/h.

We assume now that the tidal elevation can be described as a sum of cosine waves with the above frequencies, amplitudes M and S and phases α_1 and α_2 , respectively. The sum can than be expressed by:

$$h(t) = M \cos(\sigma t - \alpha_1) + S \cos((\sigma + \beta)t - \alpha_2) \quad (104)$$

We can choose now a reference time $t'=t+t_0$ for which both waves are in phase and use this to express

$$h(t') = M \cos(\sigma t' - \alpha) + S \cos((\sigma + \beta)t' - \alpha) \quad (105)$$

Further development of the right side gives:

$$h(t') = M \cos(\sigma t' - \alpha) + S \cos(\sigma t' - \alpha) \cos \beta t' - S \sin(\sigma t' - \alpha) \sin \beta t' \quad (106)$$

Which can be written as:

$$h(t') = (M + S \cos \beta t') \cos(\sigma t' - \alpha) - S \sin \beta t' \sin(\sigma t' - \alpha) \quad (107)$$

We introduce the variables R and κ such as

$$M + S \cos \beta t' = R \cos \kappa \quad (108)$$

and

$$S \sin \beta t' = R \sin \kappa \quad (109)$$

this results in

$$\operatorname{tg}\kappa = \frac{S \sin \beta t'}{M + S \cos \beta t'} \quad (110)$$

and

$$R^2 = (M + S \cos \beta t')^2 + S^2 \sin^2 \beta t' = M^2 + S^2 + 2MS \cos \beta t' \quad (111)$$

This enables us to express the combined tidal surface elevation such as:

$$h(t') = R(\cos(\sigma t' - \alpha) \cos \kappa - \sin(\sigma t' - \alpha) \sin \kappa) = R \cos(\sigma t' - \alpha + \kappa) \quad (112)$$

The above function describes a wave $h(t')$ with amplitude R which varies between $M+S$ and $M-S$ with frequency β as variation of a basic oscillation. The basic oscillation has a basic frequency σ (moons tidal wave frequency) and a periodically varying phase shift κ , varying with frequency β , resulting in a 14-daily perturbation. High water will than occur at the times

$$\sigma t' - \alpha + \kappa = n2\pi; n = 0,1,2,3,\dots \quad (113)$$

resulting in

$$\sigma t' = \alpha - \kappa + n2\pi; n = 0,1,2,3,\dots \quad (114)$$

The high water time for moons tidal wave only is given by:

$$\sigma t' = \alpha + n2\pi; n = 0,1,2,3,\dots \quad (115)$$

We investigate now the time aberration by investigation of κ . We derivate $\operatorname{tg} \kappa$:

$$\frac{d}{dt'} \operatorname{tg} \kappa = \beta \frac{MS \cos \beta t' + S^2}{(M + S \cos \beta t')^2} \quad (116)$$

Maximum values of $\kappa(t')$ occur for maximum values of $\operatorname{tg} \kappa$, hence if the derivative is zero. This occurs for

$$\cos \beta t' = -S / M = -0,46 \quad (117)$$

which results in the solution

$$\operatorname{tg} \kappa_m = \pm 0,52; \kappa_m = 27,4^\circ \quad (118)$$

Hence the maximum time deviation of the composed high water from sun and moon is 27,4 degree, which results in a time difference of

$$\frac{\kappa_m}{\sigma} = \frac{27,4^\circ}{28,984^\circ / h} \quad (119)$$

which is slightly less than an hour.

The composed wave will have a maximum amplitude for $t'=0$ (111). This is equivalent with $t=t_0$, resulting in (use 104 to derive this)

$$t_0 = \frac{\alpha_2 - \alpha_1}{\beta} \quad (120)$$

t_0 is the retardation of the spring tide after new- or full moon, as well referred to as age of the tide.

4. The geophysical phenomena of tides

Theme of our lecture is the following: after discussion of the world comprehensive tidal forcing in the first chapter, we'll now concentrate on the discussion of the geophysical phenomena of tides to form a more practical part of the discussion and investigate the tides in the real world.

4.1 Manifestation of tides in the world ocean –observation and interpretation-

Tides are a world comprehensive process which could locally create strong currents and pronounced sea level changes, particularly in the shallow part of the world ocean. In the first chapter we dealt with the theoretical understanding of tidal phenomena in general. This research has been motivated by human wish for deeper understanding of tidal phenomena itself and led to increased understanding of tidal forcing. However, soon it became clear that the regional and local response to the world comprehensive forcing strongly varies for the different parts of the ocean.

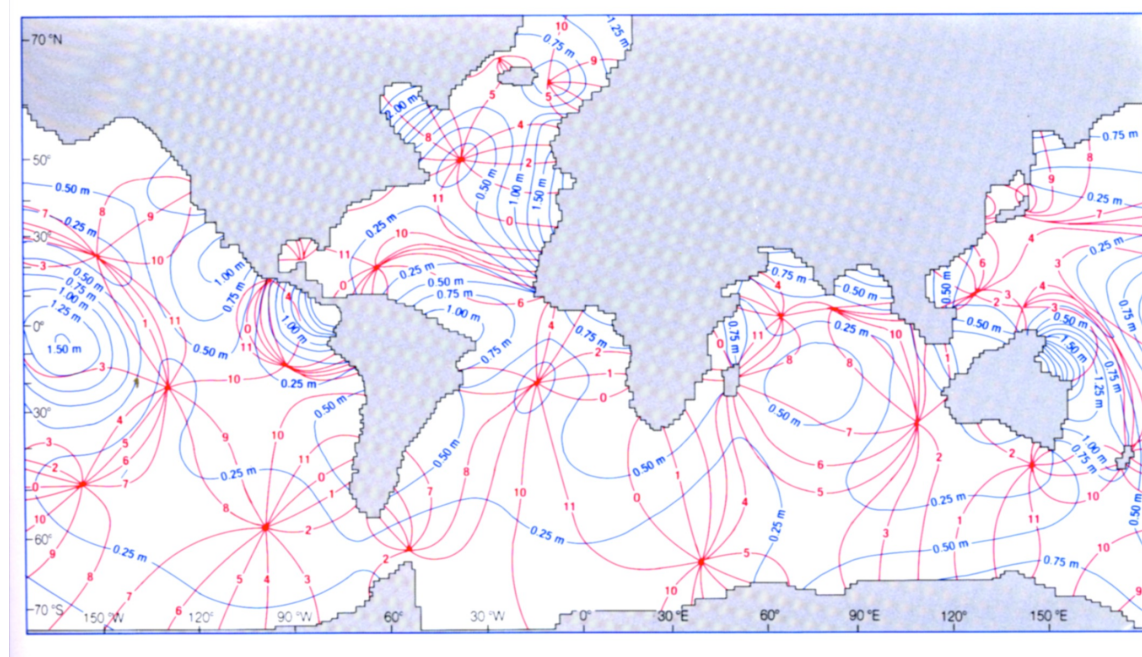


Fig.23 Computer generated diagram of world-wide amphidromic systems for the dominant semi-diurnal lunar tidal component M2. Blue lines are co-range lines and red lines are co-tidal lines, figure taken from Open University Course.

The equilibrium tidal theory, developed from Newton's theory of gravitation consists of 2 symmetric tidal bulges, directly under and directly opposite the moon or sun. Semi-diurnal tidal ranges would reach their maximum value of about 0.5 along the central line (i.e. in case of zero declination above the equator). The individual high water bulges would track around the earth, moving from E→W in steady progression. These characteristics are clearly not those of the observed tides. Consistent with equilibrium tidal theory, observed tides in the main oceans have mean ranges of about 0-1 m (amplitudes 0-0.5), but there are considerable variations (Fig. 23), which bear no relationship to the simple idea of 2 tidal bulges.

Exemplary, we can identify two significant deviations from Fig. 23:

- The tides spread from the ocean onto the surrounding shelves, where we can find much higher amplitudes, in some shelf seas, the spring tidal ranges might exceed 10 m.
- Propagation direction deviates strongly from strict E-W propagation, e.g. N-E propagation is found for the Northwest European Shelf.

We have to remind ourselves again on limitations of equilibrium tidal theory to understand these deviations:

- 1) **Assumption of water covered earth, no boundaries.**

But: Any water movements on the earth obey the physical laws represented by the hydrodynamic equations of continuity and the momentum balance (Navier-Stokes equations). Hence, the propagation of long waves and particularly any propagation from E to W would be impeded by the N-S continental boundaries. The Antarctic circumpolar region is the only area where undisturbed E-W propagation round the globe is possible.

- 2) **Tidal wave follows the earth rotation.**

But: Long waves travel at a speed given by $c = \sqrt{gH}$. Even in the absence of barriers it would be impossible for an equilibrium tidal wave to keep up with the moon's tracking. The average depth is about 4000m, resulting in a wave speed of 198 m/s. The sub-lunar point travels at an average speed of about 450 m/s at equatorial latitudes. Hence, the average wave speed is limited to less than half the speed of earth rotation. Around Antarctica however (i.e. at 60°S) both velocities are nearly identical.

3) Negligible effects of non-linearity.

But: The different ocean basins have their individual natural modes of oscillation which influence their response to the tide generating forces. The different ocean basins have their own respective resonant frequencies. In general, the ocean seems to have a resonant frequency near the semi-diurnal tidal frequency. The response to the diurnal frequency seems to be much weaker (Fig 7).

4) Rotational effects are small.

But: Rotation of the earth effects all water movements and results in deflection of movements (to the right: northern hemisphere, to the left: southern hemisphere); The idealised Kelvin Wave is the simplest model of a tidal wave propagating in a rectangular basin.

5) Furthermore: Elastic response of the solid earth to tidal forcing and additional local forcing due to tidal loads. These effects influence tidal records.

Hence to understand the geophysical tidal phenomena we have to study wave propagation, wave reflection, interference of tidal waves, the eigenmodes of ocean basins and dissipation of tidal energy.

4.2 Standing waves, resonance

The propagation of tides in the real ocean as endlessly progressive waves is impossible. They undergo reflection at sudden changes of depth and at the coastal boundaries. These reflected and incident tidal waves combine together and result in the observed tides. Consider the simplest case of a wave travelling in a long channel with one open boundary and a closed end at which the incoming wave will be reflected. The simplest case is the reflected wave and incident wave combining together without loss of amplitude (i.e. loss of energy).

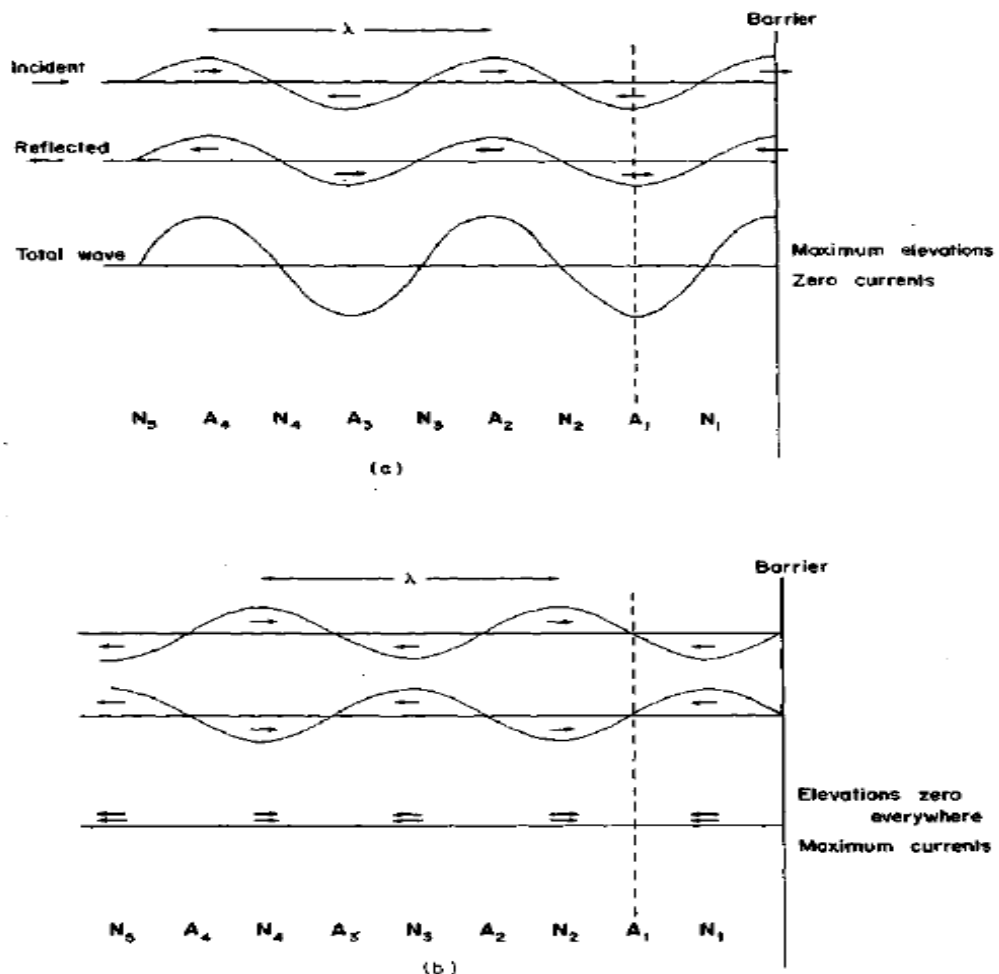


Figure 24 Incident and reflected waves of equal amplitude, which produce a standing wave pattern with nodes and antinodes. The corresponding currents are indicated by arrows. (a) High water at the reflecting barrier; (b) A quarter of a period later the incident wave has moved a quarter wavelength towards the barrier, and the reflected wave has moved a quarter wavelength in the opposite direction away from the barrier. After half a cycle the elevations and

currents are the reverse of (a); after three-quarters of a period they are the reverse of (b). Figure taken from Pugh (1996).

The interference between these 2 waves produce the pattern of a standing wave with alternating antinodes (positions where the amplitude is at maximum, each separated by a distance $\lambda/4$, with λ being the wave length of the original progressive wave). The first antinode is at $\lambda/2$ (maximum elevation similar at the boundary, zero currents). The currents alternate hence, movements across the antinodes does not develop. We could therefore simplify the description of this oscillation (once established) as a standing wave in a rectangular basin (Fig. 25).

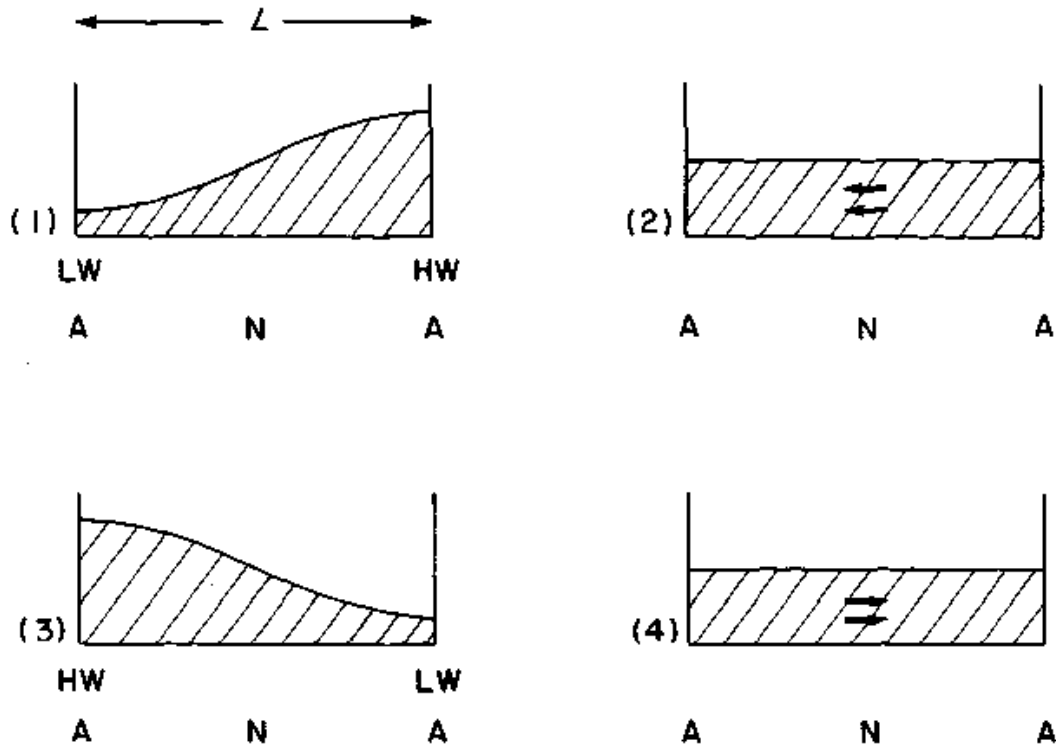


Fig. 25: First gravitational mode for oscillations of water in a closed rectangular box, showing nodes and antinodes for levels and currents (after Pugh, 1996).

The period-wave length relation for this case is given by the Merians formulae:

$$T = \frac{2 \cdot L}{\sqrt{gH}} \quad (121)$$

With L being the basin length, H the water depth and T being the period of the oscillation.

Standing waves in basins which are open at one end, occur with the double wave length. In this case, the period wave length relation is:

$$T = \frac{4 \cdot L}{\sqrt{gH}} \quad (122)$$

This model approximates the tidal behaviour in many shelf sea basins, although an exact quarter wave dimension would be very unlikely. In reality, the open boundary lies within a node or outside the node as shown in Fig. 26, but as long basin dimension/4 and the wave length have the same dimension (are similar), the probability of tidal amplification still exists. However, this is not the case anymore when the length of the basin only is a small fraction of the wave length.

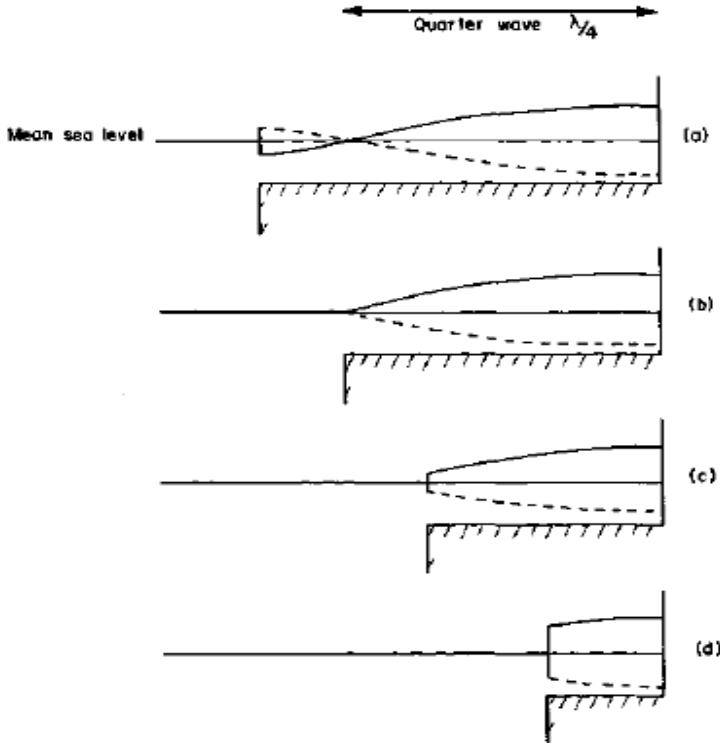


Figure 26: Responses of sea basins driven by tidal level changes at the open end, near to quarterwave resonance. There is maximum amplification when the basin length corresponds to a quarter of a tidal wavelength (adopted from Pugh, 1996).

This type of forced oscillation is different from the free seiche oscillations, which can be initiated by an impulse at the boundary and continue for a long time until damped by frictional energy loss. The forced oscillations with periods other than the seiche periods will continue only as long as the forcing at the open boundaries persists.

Systems which are forced by oscillations close to their natural period have large amplitude responses. This resonant behaviour is familiar in many physical systems. The response of oceans and many seas are close to resonance. In nature the forced resonant oscillations cannot grow indefinitely because energy loss due to friction increase more rapidly than the amplitudes of the oscillation themselves.

Water depth (m)	Basin length (km)
4000	2200
1000	1100
200	500
100	350
50	250

Table 1: Some lengths and depths of basins which would have quarter-wave resonance if driven by a semi-diurnal M2 tide.

Because of energy losses, the tidal wave is not perfectly reflected at the head of a basin, which means that the reflected wave is smaller than the ingoing wave. It is easy to show that this is equivalent to a progressive wave carrying energy to the head of the basin.

Tides in adjacent Seas

Adjacent seas are generally shallower and the water mass is small compared to the main ocean basins. This implies that the major part of the tidal energy in an adjacent basin typically is created in the open ocean. Hence, the tidal wave in an adjacent sea can be understood as a forced oscillation, we call this type of tidal phenomena co-oscillating tides; Kelvin waves are idealised models for co-oscillating tides in adjacent seas.

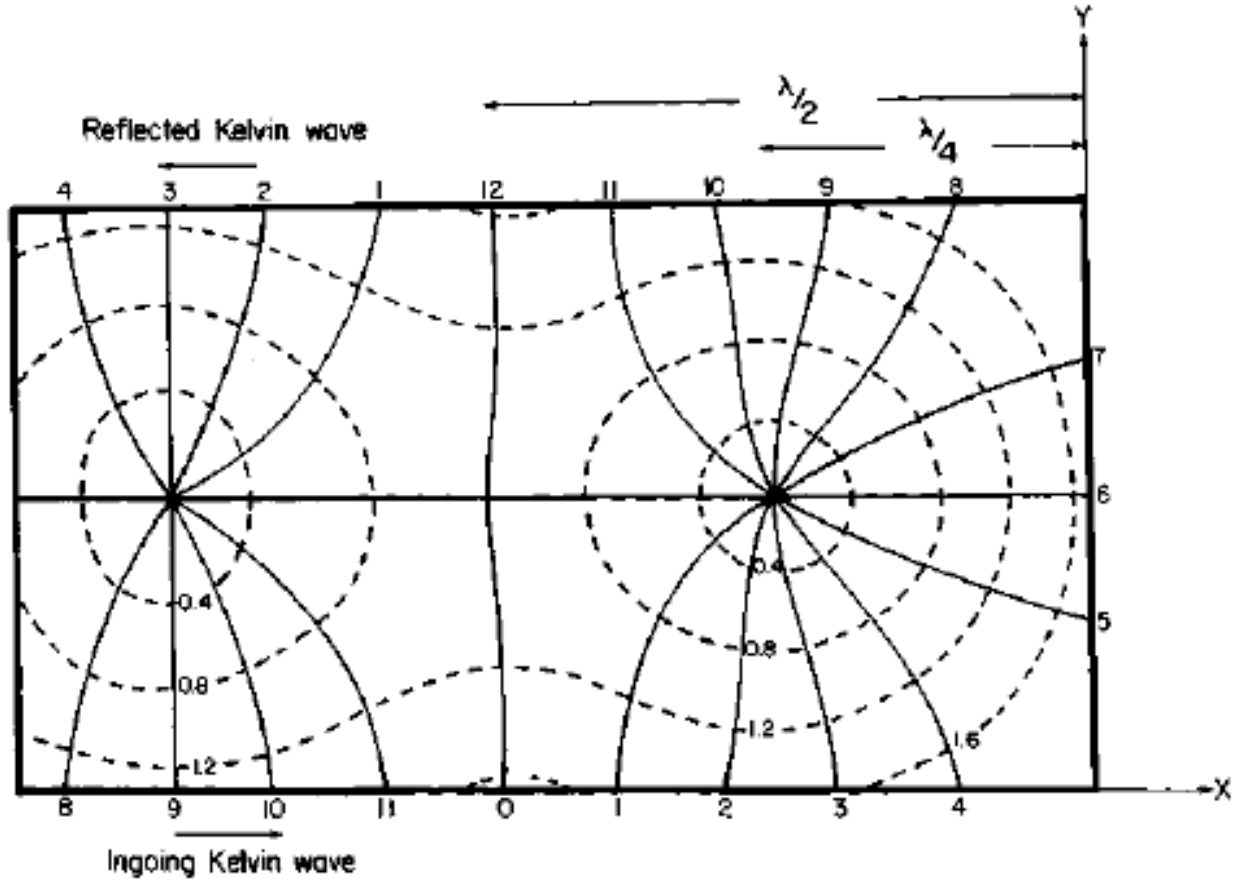


Figure 27: Cotidal and co-amplitude lines for a Kelvin wave reflected without energy loss in a rectangular channel (after Taylor 1921). Continues lines are co-tidal lines at intervals of 1/12 of a full cycle. Broken lines are lines of equal amplitude. Progression of wave crests in the northern hemisphere is anti-clockwise for both the amphidromic systems shown (Figure taken from Pugh, 1996).

Figure 27 shows an idealized superposition of 2 Kelvin waves in a rectangular channel, one incoming wave and one reflected and outgoing wave. The superposition of incoming and outgoing wave results in a tidal waves travelling around amphidromic points. The sea level shows along channel and across channel oscillations. The number of amphidromic points depend on the relation of basin length and wave length. In the idealized case, without friction, amphidromic points are located mid-channel. In case of friction cannot be neglected, the outgoing wave is less energetic (less high), and the amphidromies move to the right side of the basin, as it is the case for the North Sea system (Fig. 28+29).

4.3 Representation of tidal observations for an ocean basin or a adjacent sea

Tidal research has great practical relevance for navigation purposes. This explains the early establishment of tidal sea level stations along congested coasts and along important ship traffic lines and it motivated the observations of tidal phenomena in the open ocean and important adjacent seas, where tidal currents could get important.

During our past lessons, we learned about a number (or a hirachi) of forcing systems, with characteristic distinct periods. We found forcing with $\frac{1}{2}$ daily, daily and longer periods and learned that forcing on half daily and daily time scales occurred with a number of distinct and slightly different periods. This is very helpful for exact prognosis of tides or analysis of tidal contributions in a tidal record. However, for practical purposes semi-diurnal and diurnal components are often summarized.

Tidal observations are represented by different characteristic variables. The most common are:

- 1) Co-tidal lines, which defines high water times with respect to a well defined time.
- 2) Co-range lines → Tidal range of average variation of spring tide or double-amplitudes for single tidal constituents (e.g. M2).
- 3) Time between moons upper culmination and next high water.
- 4) Age of the tide, time delay of spring tide after new moon.
- 5) Relation between variation of nipp tide and spring tide.
- 6) Form number defining the relation between semi-diurnal and diurnal tides.

Co-tidal lines

The lines connecting points with the same high water times (co tidal lines) give an impression of wave propagation around an amphidromic point. These lines are not identical with the location of wave peaks for this time, although they are in general similar.

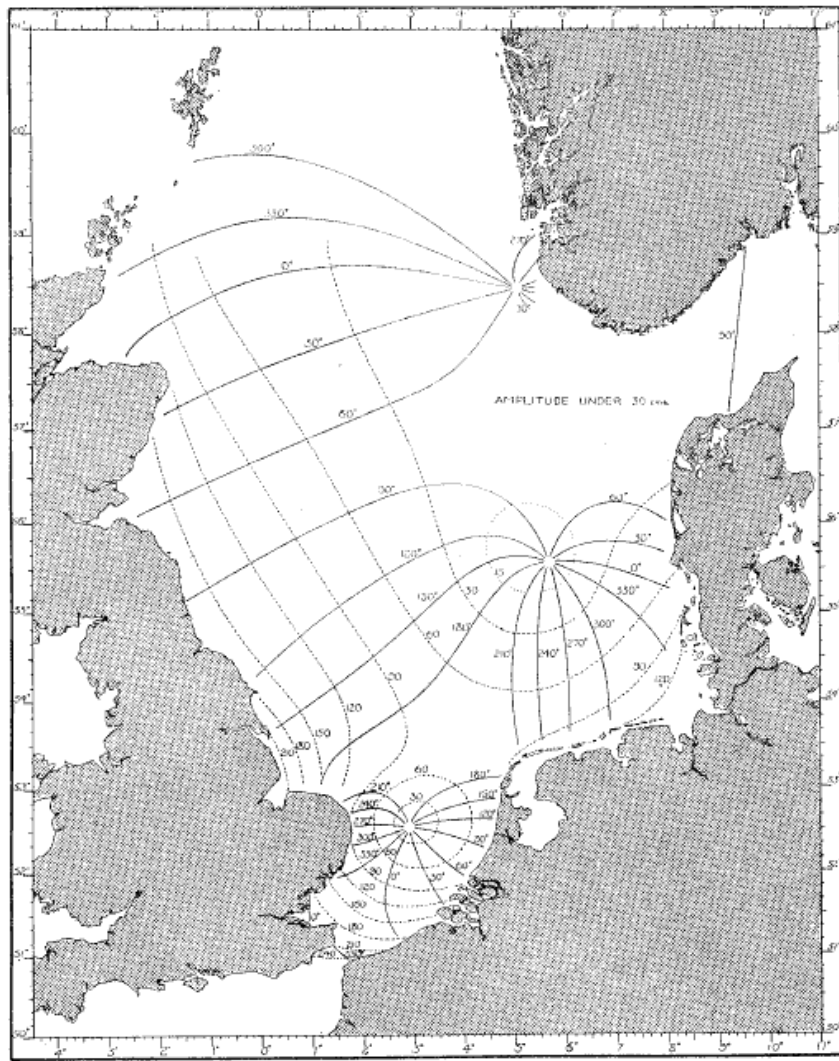


Figure 28: Co-tidal lines and co-range lines in the North Sea. Figure taken from Proudman and Doodsen (1924).

Range

The range defines normally a double amplitude for a single tidal component or an average tidal surface elevation. Amplitude isolines of a particular tidal constituent are going around the zero-elevation point in the centre of the amphidromie. Hence, the amplitudes increase with increasing distance from the amphidromic point towards the coasts and it is likely that they have a maximum near the circle line, which circumference to the original wave length. For smaller and

shallower basins, the maximum ranges are found at the coasts which is a general phenomena of Kelvin waves. Furthermore we find an influence of the coast lines, causing a retardation of wave fronts and increasing ranges, influenced by energy transfer towards the coasts.

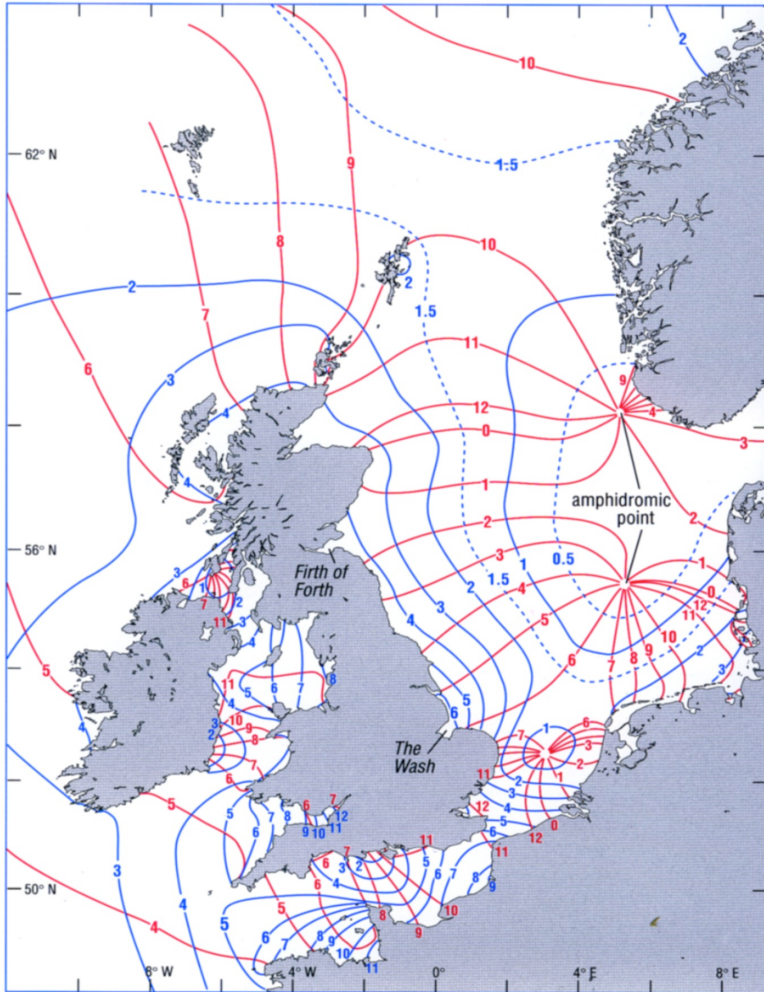


Figure 29: High water tides (in hours) after the moon passed the Greenwich meridian. Blue lines indicate co-range lines. Figure taken from Open University courses.

Mixed tidal types

The variation of the daily tidal contribution varies strongly with latitude, as we saw. Therefore it is not surprising that the tidal daily inequality shows as well strong variations with latitude, as a result of meridional variations in tidal potential and basin form. Furthermore basin form variations overlay these and the tides show strong variations as well in zonal direction. Hence it is useful to describe degree of daily inequality and we can therefore introduce the following parameter:

$$k = \frac{O_1 + K_1}{M_2 + S_2} \quad (131)$$

In the numerator we find the sum of the most important and dominating diurnal amplitudes, i.e. the main moon tide O1 and the common declination tide K1. In the denominator, the major semi-diurnal contributions of sun S2 and moon M2 are given. For the identification of different tidal forms we use the criteria:

- $k \gg 1$: mainly daily variations
- $k \ll 1$: mainly half daily variations
- $k \approx 1$: mixed tidal forms

Locations with mainly daily variations are e.g. Java → $k=3,7$; Vera Cruz → $k=5$; Mixed forms are dominating e.g. Campeche (Mexico) → 1,6 and dominating semi-diurnal variations are e.g. found e.g. for Bergen → $k=0,1$; Le Havre → $k=0,04$; Liverpool → 0,05 and Oslo → 0,13. Examples for tidal induced sea surface elevations are given in Fig. 7.

Time between moons upper culmination and next high water

Relevance first was only practical. An information of time between moons upper culmination and next high water was in previous times a relevant information for safe navigation. An example of such a chart is given in Fig. 29.

Age of the Tide

Knowledge about time lag between spring tide and new moon and relation between nipp and spring ranges were as well of practical relevance. As we will see, both phenomena are related and associated with the degree of friction and resonance in a particular basin. This applies particularly for adjacent seas where tides in general are caused by energy transfer from the deeper ocean (co-oscillating tides). In case of relative shallow adjacent seas, the incoming tidal wave will experience significant amplitudes amplification. An example is given in Fig. 30. Hence, the characteristic time lag is the result of time dependent energy transfer. We can prove that the time lag between the 2 coupled systems (incoming and outgoing wave) can reach the maximum value of $\frac{1}{4}$ of the modulation period, i.e. 3,7 days for the 14 days nipp-spring variation. For the North

Sea, the time lag (age of the tide) is about 1 and 2 days. Only for the German Bight, the age of the tide increase to about 3 days. The North Sea is of interest as well from an energetic point of view. The energy propagates into the North Sea from the Atlantic Ocean, particularly from the Norwegian Sea. Energy propagation entering the North Sea from the English Channel is much weaker. At the Utsira-Shetland section, the wave behaves nearly as progressive wave. Hence, the no or only little energy is reflected, but most of the energy is dissipated in the basin. Equilibrium state is fully defined by resonance and friction behaviour of the basin.

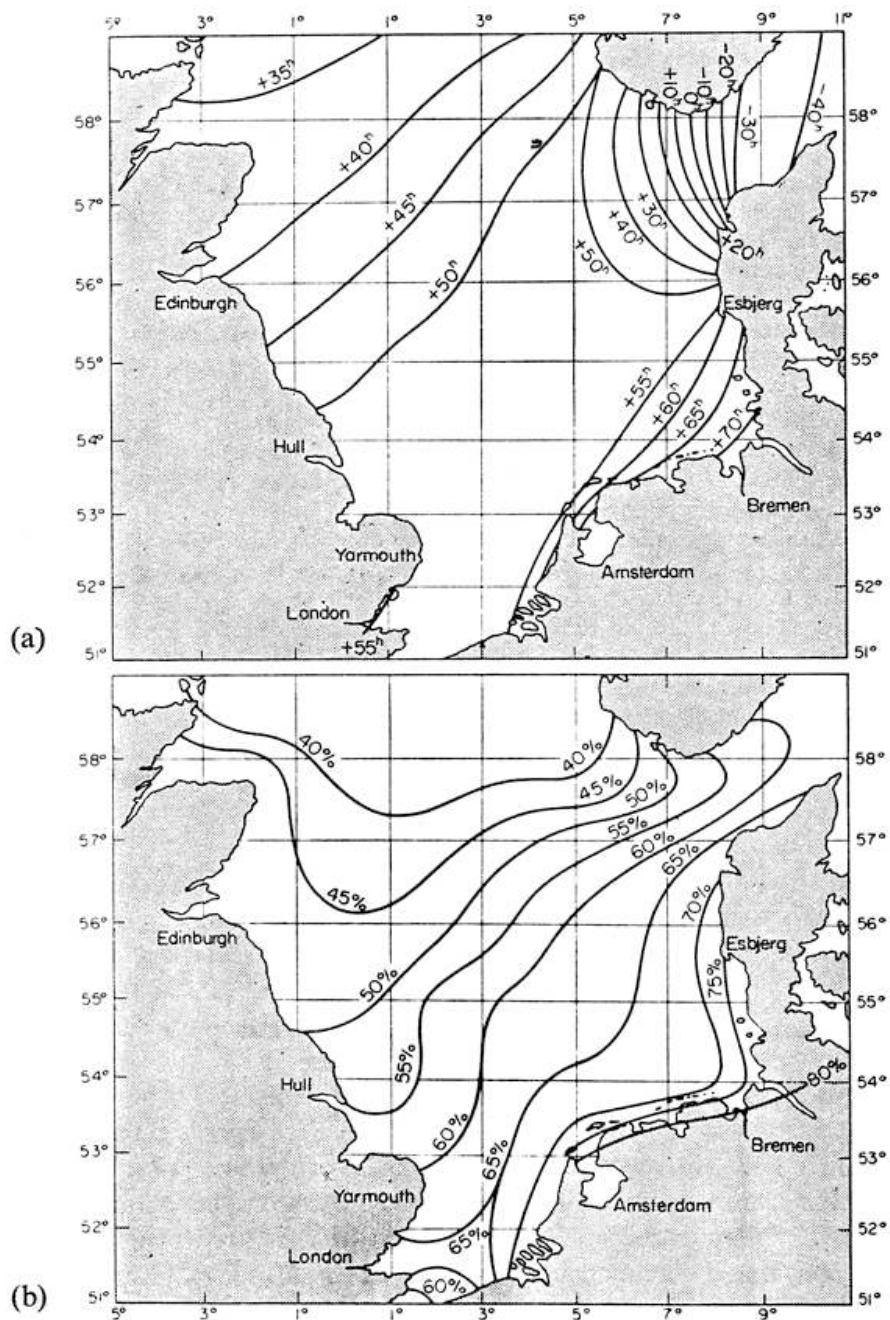


Figure 30. Properties of the North Sea tide as presented by Mertz (1923), (a) Isolines of spring tide retardment (in hours) and (b) interpolated neap to spring tide ratio. Figure taken from Gade (1998).

4.4 Theoretical formulation of neap-spring problem

An oscillating system contains energy. In case the system is coupled to another oscillating system and energy dissipation occurs due to friction, a transfer of energy between the 2 systems occurs. The energy exchange is not spontaneous, but a time dependent oscillating process. We'll study nipp-spring relation in a resonant basin with friction in an idealised model. Let us assume that the oscillation state is the consequence of a forced oscillation (P_0) and a reflected wave or natural oscillation of the basin (Q_0) with a semi-diurnal basic frequency (σ). Both are furthermore modulated by a 14-days variation (spring-neap problem, P_1 and Q_1). The function describing the sea level response inside and outside the basin, i.e. $P(t)$ and $Q(t)$ with frequency ω and phase Φ_0 are given by:

$$P(t) = P_0 + P_1 \cos \omega t \quad (123)$$

$$Q(t) = Q_0 + Q_1 \cos(\omega t - \phi_0) \quad (124)$$

We now define an energy flux $R(t)$ into the system and an energy flux out of the system $S(t)$ and assume that these are directly proportional to the respective oscillation functions (remember, energy of a wave is proportional to its amplitude), with:

$$R(t) = k_1 P(t) \quad \text{and} \quad S(t) = k_2 Q_1(t) \quad (125)$$

When integrating over one (or more) full synodic period, we could assume that the oscillation in the basin $Q(t)$ reaches a stationary state, and varies around an average mean state. Hence, an average energy balance (see Fig. 31) must exists, between incoming and outgoing energy with:

$$\overline{R(t)} = \overline{S(t)} \quad (126)$$

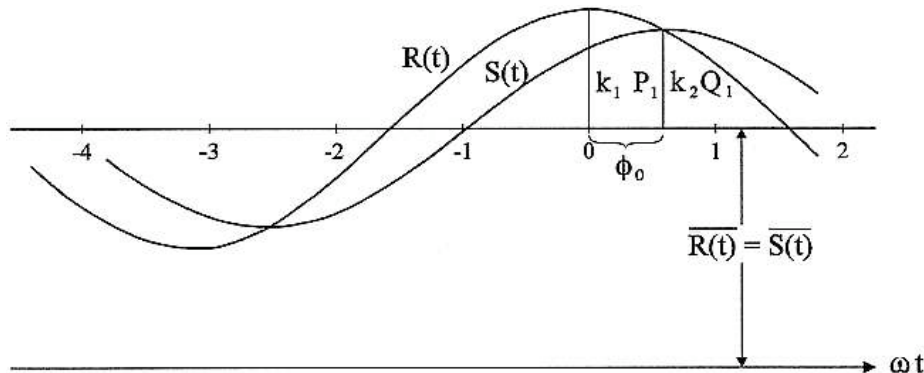


Fig. 31. Schematic presentation of energy fluxes $R(t)$ and $S(t)$ of the system and inherent phase shift of semi-monthly variation.

The two functions $R(t)$ and $S(t)$ are phase shifted with angle Φ_0 . We notice that the forcing function intersect the reflected wave in its maximum $S(t) = k_2 Q_1$. Left (before) of the shearing point, $R(t) > S(t)$ and hence a positive net energy flux towards the basin occurs. Consequently, right (or after) from the shear point $R(t) < S(t)$, hence a net energy flux from the reflected wave occurs. It follows that the shear point is a maximum value of the state function $Q(t)$ and consequently of $S(t)$. From this argument it follows:

$$\cos \phi_0 = \frac{k_2 Q_1}{k_1 P_1} \quad (127)$$

The spring-neap relation of the incoming wave:

$$\gamma = \frac{P_0 - P_1}{P_0 + P_1} \quad (128)$$

and similarly for the reflected wave:

$$\eta = \frac{Q_0 - Q_1}{Q_0 + Q_1} \quad (129)$$

From 126-129 it results that the phase shift between incoming and outgoing wave is determined by:

$$\cos \phi_0 = \frac{1 + \gamma}{1 - \gamma} \cdot \frac{1 - \eta}{1 + \eta} \quad (130)$$

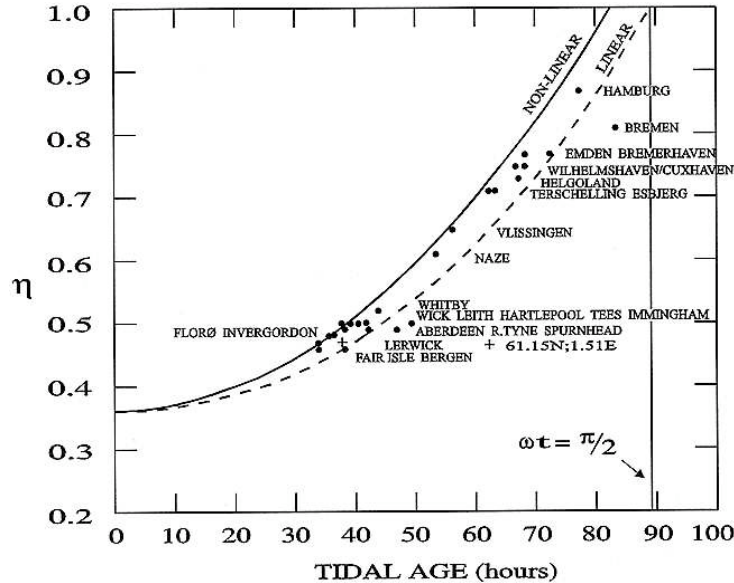


Figure 32. Functional relationship between theoretical neap to spring tide ratio and spring tide retardment according to linear theory(dashed curve) and nonlinear theory (solid curve), with observations from the North Sea against tidal age.

In Figure 32, observed neap-spring tide ratios are shown as a function of spring tide retardement for different locations in the North Sea. In addition to the observed points, 2 bounding lines are given here. The first one is estimated from linear energy transfer as discussed above, the second line was estimated assuming non-linear energy transfer, this will be discussed later. The observed points are mainly located between the two lines. It is important to note that the spring tide retardation is independent on the energy transfer coefficients k_1 and k_2 in both cases, linear and non-linear friction.